Establishing Halogen-Bond Preferences in Molecules with Multiple Acceptor Sites

Amila M. Abeysekera[a], Boris B. Averkiev [a], Abhijeet S. Sinha[a], Pierre Le Magueres[b] and Christer B. Aakeröy[a]*

[a] Dr. A.M. Abeysekera, Dr. B.B. Averkiev, Dr. A.S. Sinha, and Prof. Dr. C.B, Aakeröy, Department of Chemistry
Kansas State University
Kansas State University, 213 CBC Building, 1212 Mid-Campus Dr North, Manhattan, KS 66506-0401
E-mail: aakeroy@ksu.edu
[b] Dr. P. Le Magueres, Rigaku Americas Corporation
9009 New Trails Drive The Woodlands, TX 77381

Supporting information for this article is given via a link at the end of the document.

Abstract The interplay between hydrogen bonds (HBs) and halogen bonds (XBs), has been addressed by co-crystallizing two halogen bond donors, 1,4-diiodotetrafluorbenzene(DITFB) and 1,3,5-trifluoro-2,4,6-triiodobenzene(TITFB) with four series of targets; N-(pyridin-2-yl)benzamide (Bz-X), N-(pyridin-2-yl)picolinamides (2Pyr-X), N-(pyridin-2-yl)nicotinamides (3Pyr-X), N-(pyridin-2-yl)isonicotinamides (4Pyr-X); X=H/Cl/Br/I. The structural outcomes were compared with interactions in the targets themselves. 13 co-crystals were analysed by single-crystal X-ray diffraction (SCXRD). In all three co-crystals from the 2Pyr series, the intramolecular HB remained intact while the XB donors engaged with the N(pyr) or O=C sites. In the ten co-crystals from the other three series, the intermolecular HBs present in the individual targets were disrupted in 9/10 cases. Overall, the acceptor sites selected by the halogen-bond donors in these targets were distributed as follows; N(pyr)=81%, O=C(15%) or π (4%).

Introduction

Molecular recognition[1,2] a key concept in fundamental chemical[3] and biochemical [4,5,6,7] processes, relies on a delicate balance between molecular size,[8[shape,[9] lattice energy stabilization,[10] functional-group complementarity. In addition, the competition between a variety of directional intermolecular forces is ultimately responsible for selectivity and binding reversibility, which are key characteristics of any practically useful recognition events.[11,12,13.14,15] A subsequent transition from solution to solid-state events takes us into the realm of crystal engineering[16,17] which requires the ability to systematically assemble molecules into specific architectural features via non-covalent interactions. The most commonly utilized and best understood supramolecular synthetic driver is the hydrogen bond.[18,19] However, the halogen bond (XB)[20] and many other σ-hole interactions are also being investigated for the purpose of synthetic crystal engineering.[21] The halogen bond displays a slightly higher directionality and a larger degree of tunability than the hydrogen bond (HB),[22,23] but due to the importance of the electrostatic component in both interactions, they are capable of competing for the very same binding sites. Therefore, in order to develop more reliable and transferable protocols for supramolecular synthesis, we need to know in advance if a particular XB-donor will displace a certain HB-donor from an acceptor site. A schematic example of how the outcome of such a competition can lead to very different supramolecular assemblies is illustrated (Figure 1).

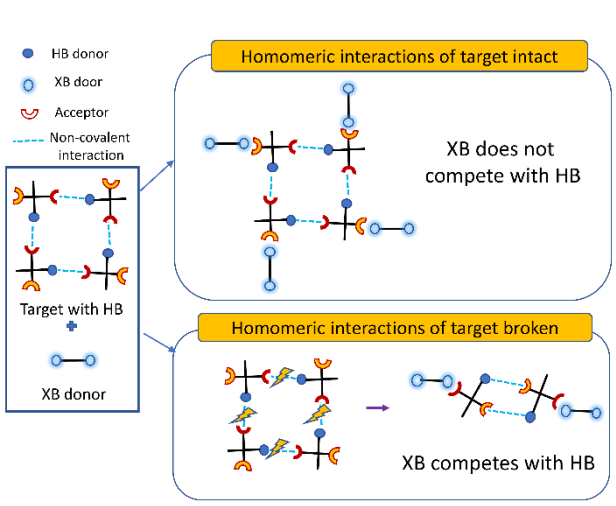

Figure 1. Postulated outcomes when a multi-functional supramolecular target is interrogated by a powerful halogen-bond donor.

In order to add more insight into the structural competition between hydrogen- and halogen bonding, we have carried out a systematic co-crystal screen of halogen-bond donors and targets carrying both nitrogen- and oxygen-based acceptor sites. The structural preferences of the targets themselves is well established,[24] which makes them a very useful starting point for attempted co-crystallizations with molecular competitors. The sixteen target molecules all contain one conventional HB donor and two or three acceptor sites, Scheme 1, and we selected two co-formers that are well known to form co-crystals with a variety of species; 1,4-diiodoterafluorobenzene[25,26] and 1,3,5-triiodo-2,4,6,-tetrafluorobenzene[27] (co-formers), (Scheme 1).

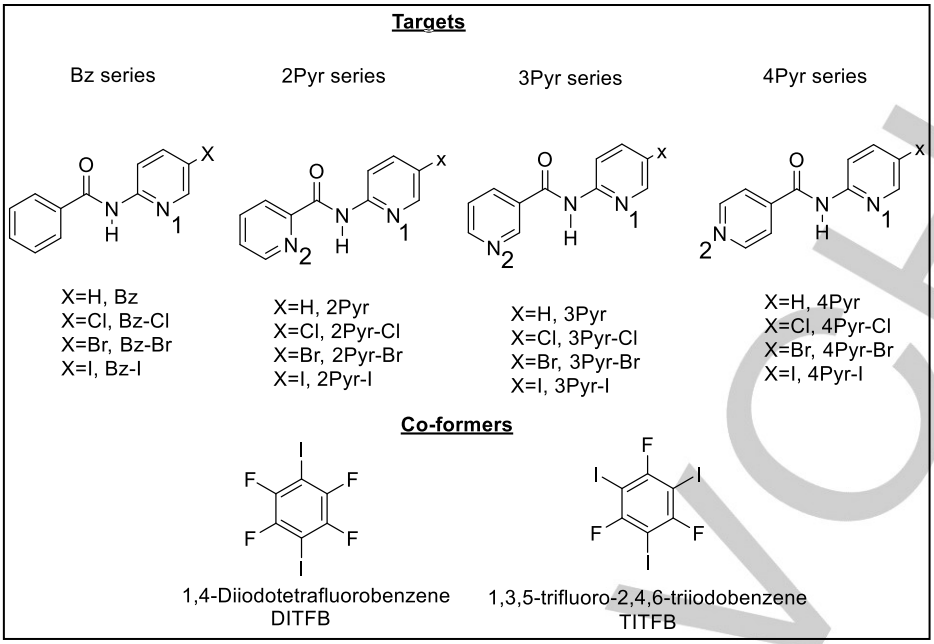

Scheme 1: Target molecules (top) and co-formers (bottom) in this study.

The sixteen target molecules offer the advantage of being equipped with a carbonyl oxygen, an acceptor site which has not been frequently utilized for assessing XB binding preferences (such investigations have mostly included nitrogen containing heterocycles as potential acceptors).[28,29] The crystal structures of the individual targets have previously been investigated[24] and the compounds in the Bz series form −NH···N_1 dimers, the 2Pyr molecules form −NH···N_2 intramolecular hydrogen bond, whereas both the 3Pyr and the 4Pyr molecules form −NH···N_2 hydrogen-bonds (with the exception of 4Pyr-I which produced either an NH···N_1 dimer (Form I) or an NH···O=C interaction (Form II). As a result, we can postulate which kind of binding sites may be targeted by the XB donors in the study presented herein (Figure 2).

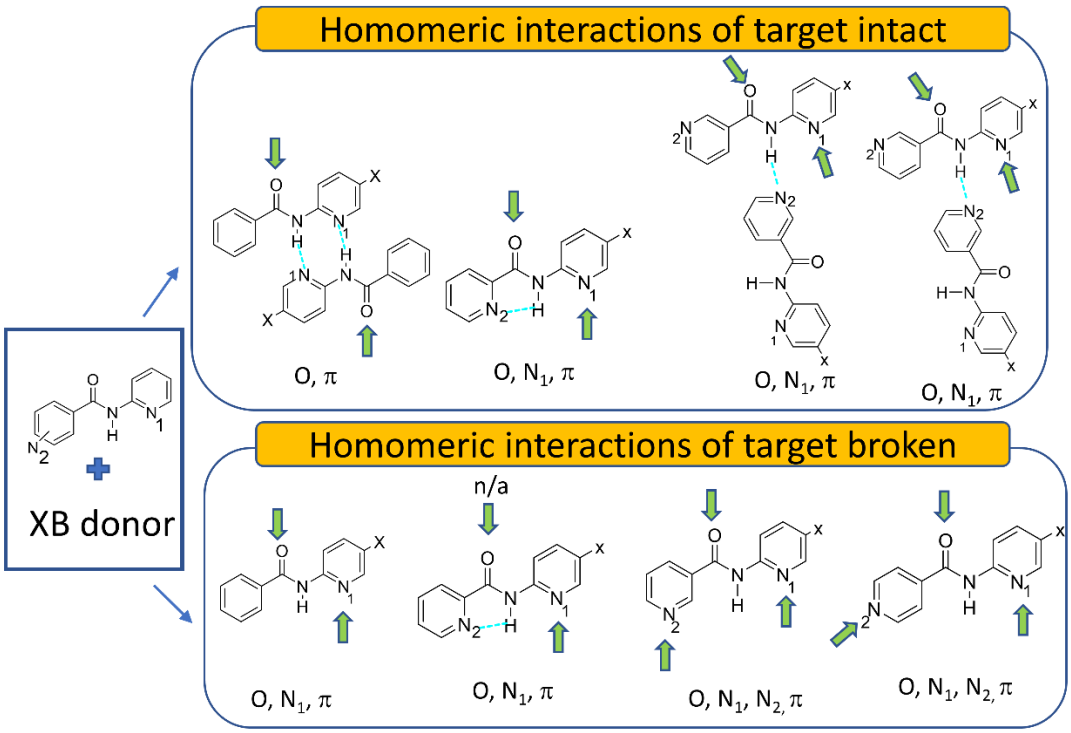

Figure 2. Possible acceptor sites on the targets that can be occupied by XB donors.

In this study we address the following questions;

1. Does the XB donor favor a specific acceptor type, *i.e.* oxygen, nitrogen or π system?
2. Are the hydrogen bonds observed in the target structures broken or intact in the resulting co-crystals?
3. Can we use any vibrational spectroscopic signatures to identify key structural features in the halogen-bonded co-crystals?

Results and Discussion

All the 32 co-crystal screening experiments gave a positive result as determined by IR spectroscopy. The relevant IR data is provided in the Supplementary Materials. The ground solids were dissolved in methanol to obtain crystals of diffraction quality. A total of 13 experiments produced crystals suitable for single-crystal X-ray diffraction (SCXRD), (Table 1).

Table 1 Some physical properties of the co-crystals obtained

Co-Crystal	Code	Melting Point	Color and Morphology
(N-(pyridin-2-yl)benzamide)1,4Diiodotetrafluorobenzene (1:1)	Bz:DITFB	88–90 °C	Colorless, Plate
(N-(pyridin-2-yl)benzamide)1,3,5-trifluoro-2,4,6-triiodobenzene (1:1)	Bz:TITFB	98–100 °C	Colorless, Plate
(N-(5-iodopyridin-2-yl)benzamide)1,4Diiodotetrafluorobenzene (2:1)	Bz-I:DITFB	165–165 °C	Colorless, Block
(N-(pyridin-2-yl)picolinamide)1,4Diiodotetrafluorobenzene (1:1)	2Pyr:DITFB	85–87 °C	Colorless, Block
(N-(5-bromopyridin-2-yl)picolinamide)1,4Diiodotetrafluorobenzene (2:1)	2Pyr-Br:DITFB	141–143 °C	Colorless, Rectangular
(N-(5-iodopyridin-2-yl)picolinamide)1,4Diiodotetrafluorobenzene (2:1)	2Pyr-I:DITFB	137–139 °C	Colorless, Rectangular
(N-(pyridin-2-yl)nicotinamide)1,4Diiodotetrafluorobenzene (1:1)	3Pyr:DITFB	110–112 °C	Colorless, Needle
(N-(5-iodopyridin-2-yl)nicotinamide)1,4Diiodotetrafluorobenzene (1:1)	3Pyr-I: DITFB	178–180 °C	Colorless, Parallelepiped
(N-(5-iodopyridin-2-yl)nicotinamide)1,3,5-trifluoro-2,4,6-triiodobenzene (1:1)	3Pyr-I:TITFB	180–182 °C	Colorless, Needle
(N-(pyridin-2-yl)isonicotinamide)1,4Diiodotetrafluorobenzene (1:1)	4Pyr:DITFB	110–112 °C	Colorless, Needle
(N-(pyridin-2-yl)isonicotinamide) 1,3,5-trifluoro-2,4,6-triiodobenzene (1:1)	4Pyr:TITFB	135–137 °C	Colorless, Plate
(N-(5-chloropyridin-2-yl)isonicotinamide)1,3,5-trifluoro-2,4,6-triiodobenzene (1:1)	4Pyr-Cl:TITFB	149–151 °C	Colorless, Needle
(N-(5-bromopyridin-2-yl)isonicotinamide)1,4Diiodotetrafluorobenzene (1:1)	4Pyr-Br:TITFB	154–155 °C	Colorless, Needle

Three co-crystals of Bz targets suitable for single-crystal X-ray diffraction (SCXRD) were successfully grown. In the two co-crystals obtained from the non-halogenated target, Bz:DITFB and Bz:TFTIB (Figure 3a-b), the homomeric N-H···N_1(py)/N_1(py)···H-N interactions present in the structure of the target itself are broken.

In Bz:DITFB, C-I···N_1 and C-I···π halogen bonds are observed, resulting in chains. The N-H···O=C hydrogen bond connects neighboring chains into an infinite 2-D architecture. In the crystal structure of Bz:TFTIB, alternating C-I···O=C and C-I···N_1 halogen bonds connect target and co-former into chains. Only two of the three iodine atoms of the co-former act as XB donors, a behavior which is relatively common.[30] Theoretical calculations on molecules with multiple halogen bond donors have shown proressive weakening of the sigma hole and subsequent halogen-bond forming ability once the first halogen bond is formed.[31] This is essentially a cooperative effect due to the donation of electron density to the first halogen-bond donor which then lowers the positive potential on the remaining donors.[32] Finally, there is also an N-H···I hydrogen bond in this structure; the negative equatorial "belt" of the iodine atom acts as the acceptor site.[33]

In the crystal structure of Bz-I:DITFB (Figure 3c), a C-I···O=C halogen bond is observed (the two iodine atoms are crystallographically equivalent), while the homomeric H···N_1(py)/N_1(py)···H-N motif, which was found in the structure of the target, remains intact. In addition, the iodine atom of the target molecule is oriented towards the negative belt of the iodine atom of the co-former in a Type II halogen bond.[34] The relevant hydrogen- and halogen-bond geometries in the three co-crystals from the Bz series are given (Table 2)

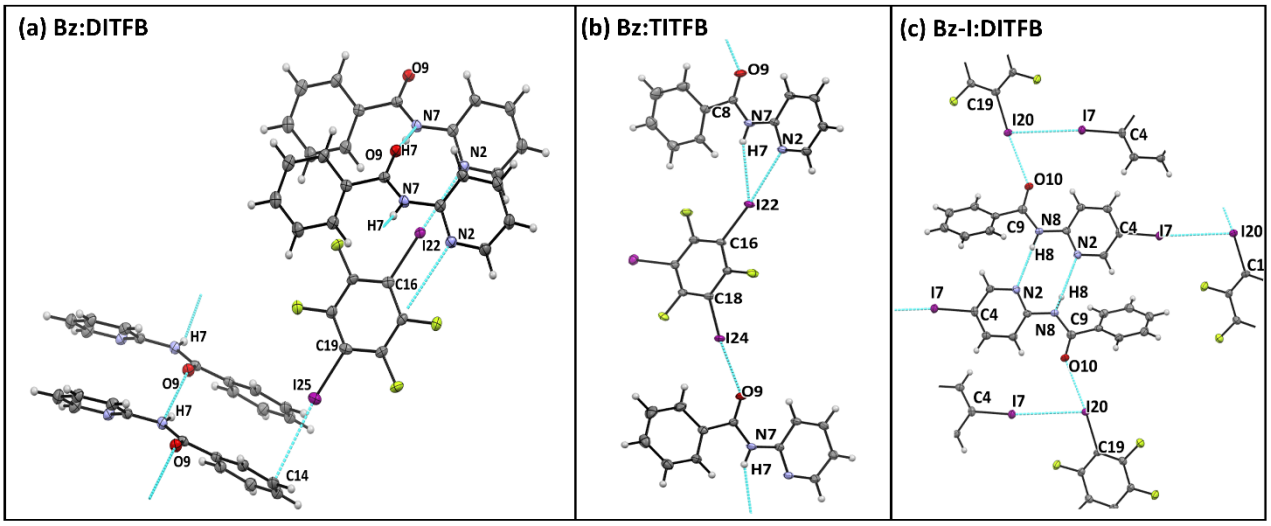

Figure 3. Primary interactions in crystal structures of (**a**) Bz:DITFB, (**b**) Bz:TITFB, and (**c**) Bz-I :DITFB.

Table 2 Hydrogen- and halogen-bond parameters in the three Bz series co-crystals.

Co-crystal	D-H/X··A	D/X···A (Å)	D-H/X···A (deg)
Bz:DITFB	C16-I22···N2	2.820(3)	179.03(2)
	N7-H7···O9	2.947(4)	147.0(2)
	C19-I25···C14	3.296(4)	143.49(2)
Bz:TITFB	C16-I22···N2	2.860(2)	174.96(6)
	N7-H7···I22	3.636(2)	139.45(3)
	C18-I24···O9	2.911(1)	174.28(1)
Bz-I:DITFB	C19-I20···O18	2.830(3)	174.07(1)
	N8-H8···N2	3.064(4)	167.13(2)
	C4-I20···I7	3.939(3)	170.41(1)

Three crystal structures of co-crystals of 2Pyr targets were obtained (Figure 4a-c). As expected, the homomeric −NH···N_2 intramolecular hydrogen bond of the target compounds remained intact in all three co-crystals and halogen bonding occured to the "vacant" nitrogen/oxygen atoms in the target molecule. In 2Pyr-DITFB, alternating C-I···O=C and C-I···N_1 link the target and co-former into infinite chains. The two co-crystals of 2Pyr-Br:DITFB and 2Pyr-I:DITFB are isostructural and the co-former is residing on an inversion center resulting in a 2:1 stoichiometry between target and co-former. Both iodine atoms of DITFB form C-I···N_1 halogen bonds. The relevant hydrogen- and halogen-bond geometries in the three co-crystals from the 2Pyr series are given (Table 3).

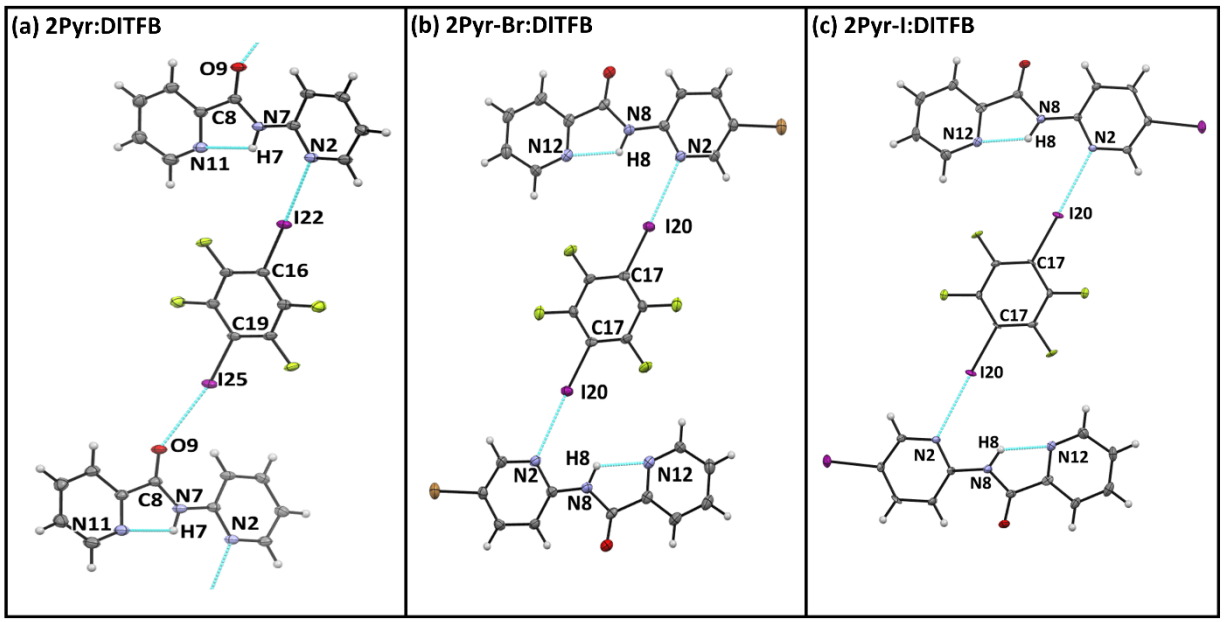

Figure 4. Primary interactions in crystal structures of (**a**) 2Pyr:DITFB, (**b**) 2Pyr-Br:DITFB, and (**c**) 2Pyr-I:DITFB

Table 3 Hydrogen- and halogen-bond parameters in the three 2Pyr series co-crystals

Co-crystal	D-H/X··A	D/X···A (Å)	D-H/X···A (deg)
2Pyr:DITFB	N7-H7···N11	2.615(3)	113.07(2)
	C16-I22···N2	2.847(2)	177.64(8)
	C9-I25···O9	2.984(2)	167.11(7)
2Pyr-Br:DITFB	N8-H8···N12	2.615(7)	118.(5)
	C17-I20···N2	2.921(2)	177.74 (1)
2Pyr-I:DITFB	N8-H8···N12	2.600(7)	121.(6)
	C17-I20···N2	2.925(6)	178.40(2)

Three crystal structures of co-crystals of 3Pyr targets were obtained (Figure 5a-c). In all three, the homomeric NH···N_2(py) interactions present in the structure of the target itself are broken. In the structure of 3Pyr:DITFB, both iodine atoms form C-I···N_1 and C-I···N_2 halogen bonds leading to the formation of tetrameric rings (Figure 5a). Additionally, the N-H···O=C hydrogen bond connect tetramers into a ladder like architecture. The crystal structure of 3Pyr-I:DITFB is isostructural with 3Pyr:DITFB. In the structure of 3Pyr-I:TITFB, C-I···N_1 and C-I···N_2 interactions are formed by a linking co-former which leads to infinite chains. Once again, the hydrogen bond motif N-H···O=C leads to stacking of chains. In addition, the third iodine atom of the co-former TITFB (which does not interact with the target molecule), forms a Type II halogen bond of van der Waals reduction of ~7%, to the Iodine atom forming a XB bond to N_2. The relevant hydrogen- and halogen-bond geometries in the three co-crystals from the 3Pyr series are given (Table 4).

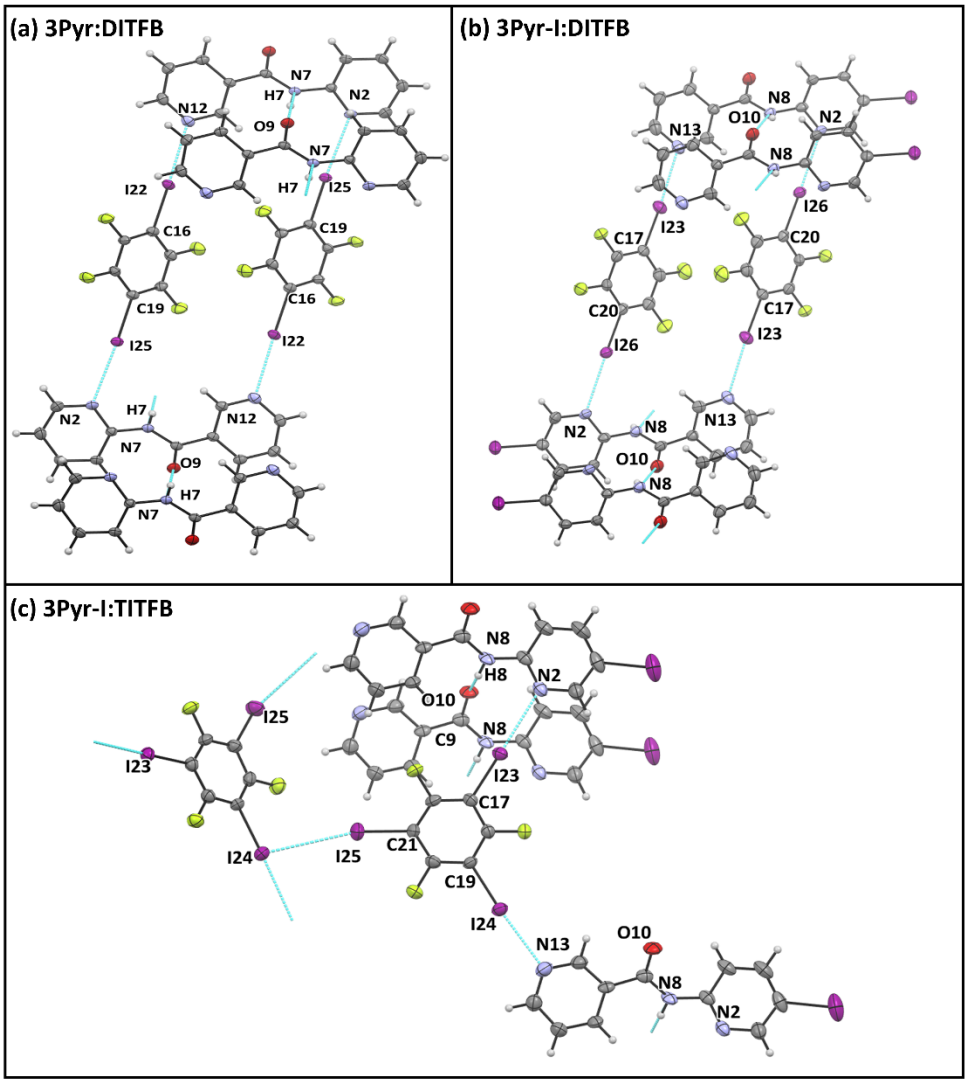

Figure 5. Primary interactions in crystal structures of (**a**) 3Pyr:DITFB, (**b**) 3Pyr-I:DITFB, and (**c**) 3Pyr-I:DITFB

Table 4 Hydrogen- and Halogen-bond Parameters in the three 3Pyr series co-crystals

Co-crystal	D-H/X··A	D/X···A (Å)	D-H/X···A (deg)
3Pyr:DITFB	N7-H7···O9	3.022(4)	151.00(1)
	C16-I22···N12	2.820(2)	178.56(7)
	C19-I25···N2	2.892(2)	177.12(7)
3Pyr-I:DITFB	N7-H7···O9	2.984(9)	150.(9)
	C17-I23···N13	2.839(7)	176.7(2)
	C20-I26···N2	2.939(6)	178.3(2)
3Pyr-I:TITFB	N8-H8···O10	2.907 (7)	143.87 (1)
	C19-I24···N13	2.830 (1)	175.67 (2)
	C17-I23···N2	2.913 (6)	179.26(2)
	C21-I25···I24	3.704 (1)	164.45 (2)

Four crystal structures of co-crystals of 4Pyr targets were obtained (Figure 6a-d). In all four, the homomeric NH···N_2 interactions present in the structure of the target itself are broken. In 4Pyr:DITFB, both iodine atoms form C-I···N_1 and C-I···N_2 halogen bonds with different target molecules leading to the formation of "z" shaped chains (Figure 6b). These chains are cross-linked by N-H···O=C hydrogen bonds (with stacking of like molecules). In 4Pyr:TFTIB, two of the iodine atoms form C-I···N_1 and C-I···N_2 halogen bonds, leading to the formation of tetrameric rings. These tetrameric rings stack while there is also

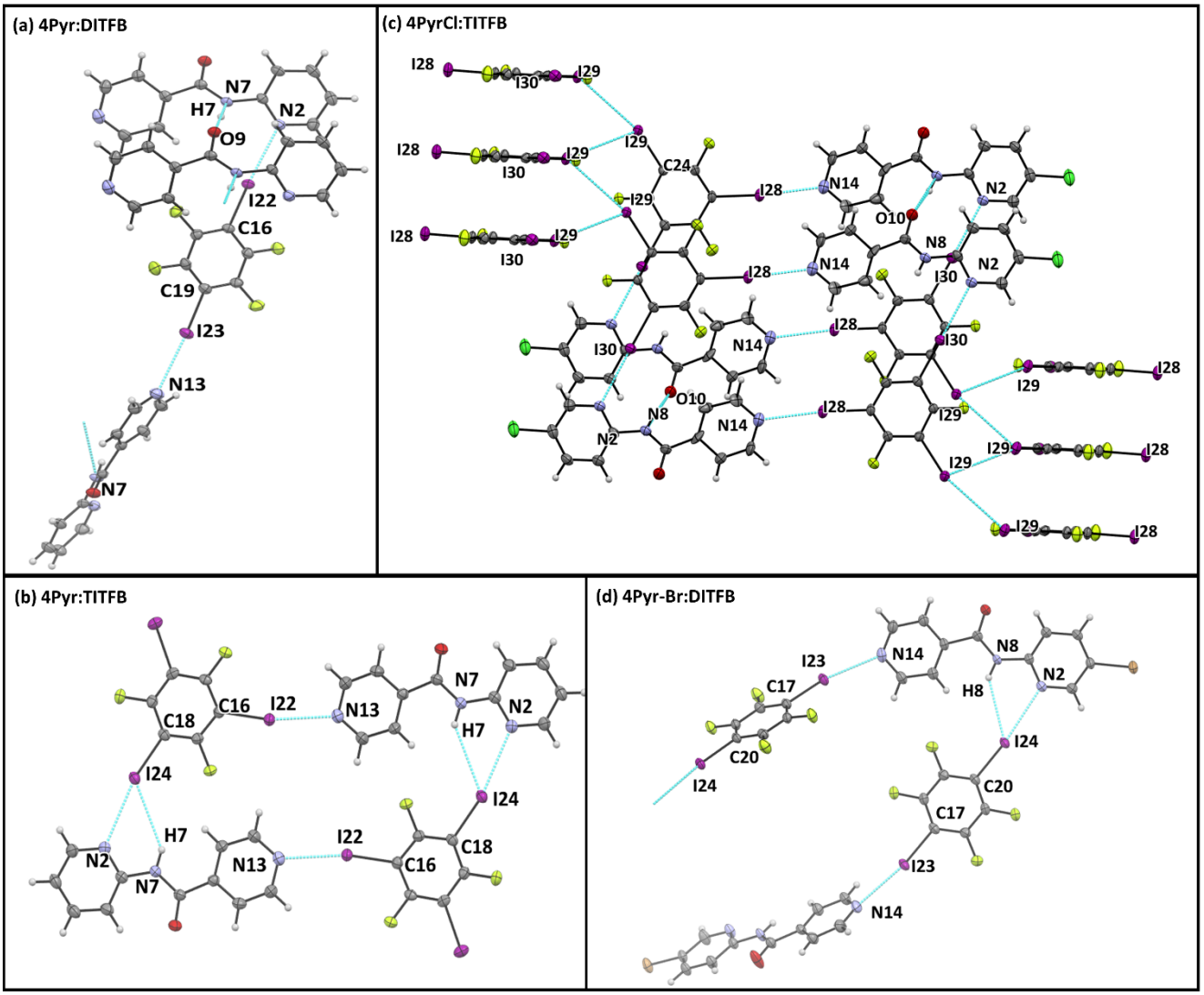

Figure 6: Primary interactions in crystal structures of (a) 4Pyr:DITFB, (b) 4Pyr:DITFB, (c) 4Pyr-Cl:DITFB, and (d) 4Pyr-Br:DITFB

an N-H···I hydrogen bond in this structure; the negative equatorial "belt" of the iodine atom acts as the acceptor site. In the co-crystal of 4Pyr-Cl:TFTIB, again two iodine atoms form C-I···N_1 and C-I···N_2 halogen bonds leading to the formation of tetrameric rings. The stacked tetrameric rings are cross-linked by NH···O=C interactions. In 4Pyr-Br:DITFB C-I···N_1 and C-I···N_2 halogen bonds lead to chain formation. The chains arrange in a spiral fashion (with target and co-former molecules stacking over targets and co-formers respectively). There is also an N-H···I interaction, to the negative belt of the iodine atom.
The relevant hydrogen- and halogen-bond geometries in the three co-crystals from the 4Pyr series are given (Table 5).

Table 5 Hydrogen- and Halogen-bond Parameters in the four 4Pyr series co-crystals

Co-crystal	D-H/X··A	D/X···A (Å)	D-H/X···A (deg)
4Pyr:DITFB	N7-H7···O9	2.916 (2)	146.76(1)
	C16-I22···N2	2.865 (2)	175.41(5)
	C19-I23···N13	2.900(2)	171.48(5)
4Pyr:TITFB	N7-H7···I24	3.750(3)	141.4(2)
	C18-I24···N2	3.000(4)	167.50(1)
	C16-I22···N13	2.813(4)	168.85(1)
4Pyr-Cl:TITFB	N8-H8···O10	2.986(6)	160.03(5)
	C22-I28···N14	2.845 (4)	174.70(1)
	C26-I30···N2	2.894 (4)	179.20 (1)
	C24-I29···I29	3.839 (4)	153.24 (5)
4Pyr-Br:DITFB	N8-H8···I24	3.696 (8)	141.61 (1)
	C20-I24···N2	2.973 (6)	173.561(2)
	C17-I23···N14	2.882(6)	168.80 (4)

It was previously noted by Ho and co-workers that the relationship between halogen- and hydrogen bonds is somewhat "schizophrenic, being competitive, complimentary or orthogonal, depending on the situation"[35]. Additionally, it has also been shown by both experimental and theoretical studies that hydrogen bonding can be used for pre-organization[36] of halogen bond donors while exerting a synergistic effect to halogen bonding.[37] In co-crystals of amide containing molecules with halogen bond donors it has been shown that the hydrogen bonding motif (amide chain) is present while the halogen bond donor bound to the carbonyl oxygen and thus these systems exhibited XBs orthogonal to HB. [38] In this family of compounds as expected, the intramolecular hydrogen bonding was intact in co-crystal of 2Pyr series targets. Considering the 10 co-crystals obtained from targets exhibiting intermolecular hydrogen bonding (Bz, 3Pyr and 4Pyr series) in the homomeric state, the prevalent intermolecular interactions of homomeric assembly was broken 9/10 times (Figure 7) *i.e.*halogen bonding competed with the hydrogen bonding. Previous studies focused on assessing the relationship (or competitiveness) between HBs and XBs have investigated systems where both the hydrogen and halogen-bond donors were located on the same molecular backbone. These test molecules were then co-crystallized with either monotopic[39] or multitopic acceptor molecules(co-formers).[40]The persistence (or otherwise) of a hydrogen bond motif was found to depend on the balance between the acceptor sites introduced in co-crystallization. For example, the acid dimer remained intact in the 4-iodotetrafluorobenzoic acid:1,4-dithiane co-crystal, but it was abandoned in the structure of the 4-iodotetrafluorobenzoic acid:thiomorpholine co-crystal[39]. In studies where multitopic acceptors were examined, it was noted that hydrogen bonding occurred to the better (more electronegative) acceptor, while halogen bonding occurred to the second-best acceptor. Interestingly, in those target molecules, the intermolecular hydrogen bond motifs were quite readily broken (9/10) upon co-crystal formation.[35]

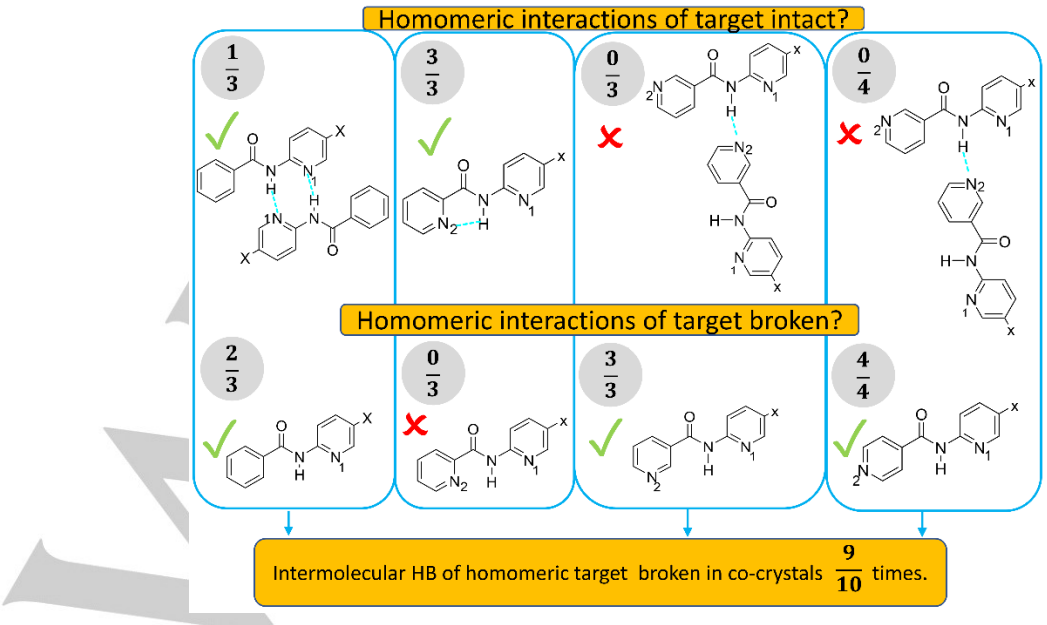

Figure 7. Summary of outcomes to HB interactions in target upon co-crystal formation

In the nine cases where the intermolecular N-H···$N_{1/2}$ motif was broken, either a N-H···O=C or N-H···I, interaction was formed instead. In all four crystals obtained with TITFB only two of the iodine atoms formed halogen bonds with the target. In all co-crystals obtained with DITFB both iodine atoms formed halogen bonds with the target molecule. Thus, in all 13 structures combined, a total 26 XBs are formed between the targets and XB donor. The majority of the time XB bond formation was to a pyridyl nitrogen (21/26), while the carbonyl oxygen was the next most popular site (4/26) and halogen bonding to π system occurring only once (1/26) (Figure 8).

The key vibrational (IR) changes observed in the ground mixtures, when compared to the analogous modes in the target structures, and between the target and co-former in the co-crystals, are summarized (Table 6).

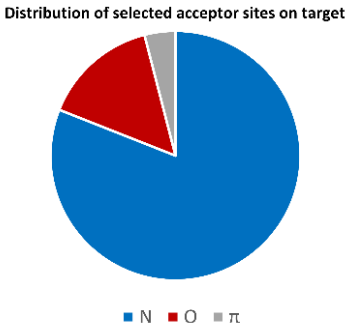

Figure 8. Distribution of selected acceptor sites on target

Table 6 Summarized IR data and interactions in targets and co-crystals

Target	Main HB in target itself	Location of IR bands for N-H, and C=O modes, respectively [cm^{-1}].	Co-Crystal	Are HBs of target changed when co-crystal is formed?	Primary interactions in co-crystal	Key IR peak positions in co-crystal for NH and O=C. [cm^{-1}]	Relative change of key IR positions in co-crystal vs. target	Acceptor site selected by XB donor
Bz	−NH···N_1	[a], 1669	Bz:DITFB	Yes	C-I···N_1 C-I···π N-H···O=C	3338, 1656	[*],-13	N_1, π
Bz	−NH···N_1	[a], 1669	Bz:TITFB	Yes	C-I···O=C C-I'···N_1 N-H···I'	3410, 1672	[*], +3	O, N_1
Bz-I	−NH···N_1	[a], 1672	Bz-I:DITFB	No	C-I···O=C	a, 1667	[**], -5	O, O
2Pyr	−NH···N_2 (intramolecular)	3342, 1686	2Pyr:DITFB	No	C-I···O=C C-I···N_1	3285, 1682	-57, -4	O, N_1
2Pyr-Br	−NH···N_2 (intramolecular)	3344, 1691	2Pyr-Br:DITFB	No	C-I···N_1 C-I···N_1	3286, 1694	-58, +3	N_1, N_1
2Pyr-i	−NH···N_2 (intramolecular)	3350 and 3331, 1689 and 1683	2Pyr-I:DITFB	No	C-I···N_1 C-I···N_1	3290, 1692	-60 and -41, +3 and +9	N_1, N_1
3Pyr	−NH···N_2	[a], 1670	3Pyr:DITFB	Yes	C-I···N_1 C-I···N_2 N-H···O=C	3326, 1653	[*], -17	N_1, N_2
3Pyr-I	−NH···N_2	[a], 1669	3Pyr-I: DITFB	Yes	C-I···N_1 C-I···N_2 N-H···O=C	3324, 1650	[*], -19	N_1, N_2
3Pyr-I	−NH···N_2	[a], 1669	3Pyr-I:TITFB	Yes	C-I···N_1 C-I···N_2 N-H···O=C	3317, 1655	[*], -14	N_1, N_2
4Pyr	−NH···N_2	[a], 1684	4Pyr:DITFB	Yes	C-I···N_1 C-I···N_2 N-H···O=C	3298, 3271, 1669	[*], -15	N_1, N_2
4Pyr	−NH···N_2	[a], 1684	4Pyr:TITFB	Yes	C-I'···N_1 C-I···N_2 N-H···I'	3284, 1659	[*], -25	N_1, N_2
4Pyr-Cl	−NH···N_2	[a], 1678	4Pyr-Cl:TITFB	Yes	C-I···N_1 C-I···N_2 N-H···O=C	3388, 1693	[*], +15	N_1, N_2
4Pyr-Br	−NH···N_2	[a], 1680	4Pyr-Br:DITFB	Yes	C-I'···N_1 C-I···N_2 N-H···I'	3403, 1686	[*], +6	N_1, N_2

[a]= not detectable. [*] = emergence/defining of a new peak, [**]=unchanged

In two of the three co-crystals from the Bz series the homomeric dimeric NH···N_1 hydrogen bonding in the target structure was broken in co-crystal formation. In these two co-crystals Bz:DITFB and Bz:TITFB the pyridyl nitrogen N_1 was selected by one of the XB donor atoms while the second donor site of XB donor bound to a different site (either carbonyl oxygen or π cloud in the target molecule). The net change in O=C position in IR was higher when a NH···O=C interaction (-/Δ 13, in Bz:DITFB) in comparison to when a C-I···O=C (+/Δ 3, Bz:TITFB) was formed with the same target molecule. In the instance of Bz-I:DITFB, where the homometic HB remained unchanged, with I···O=C halogen bond formation there was no discernible changes observed in the amide region of co-crystal IR spectra while the carbonyl peak shifted by (+/Δ 5).Thus, in the two cases where the hydrogen bond motif was changed, the IR at amide position visibly altered by the emergence of an NH peak which was not seen in spectra of the individual target compound, Bz.

As expected, the intramolecular hydrogen bonding of the targets in 2Pyr series remained intact in co-crystal formation. Halogen bonding occurred to the vacant N_1, nitrogen atom 5/6 times. In the one instance, 2Pyr-I:DITFB where a C-I···O occurred could be result of the higher negative charge of the carbonyl oxygen of the 2Pyr target in comparison to 2Pyr-Br and 2Pyr-I. Due to the difference in selected binding sites, although the ratio in the solution of target:co-former was 1:1 in all three cases, the co-crystal stoichiometry was 1:1, 2:1 and 2:1 in 2Pyr:DITFB, 2Pyr-Br:DITFB and 2Pyr-I:DITFB respectively. All three co-crystals were accompanied by a significant red shift of the amide NH of ~60.

In the crystal structures of 3Pyr:DITFB, 3Pyr-I:DITFB and 3Pyr-I:TITFB, the HB in the target was altered from −NH···N_2 to N-H···O=C. Halogen bonding occurred at both pyridyl nitrogen sites N_1 and N_2. In all three co-crystals, the carbonyl peak in the IR spectrum was red shifted in the range of ~14-19 and lead to an emergence of NH peak which was not seen in spectra of individual target molecule.

In the crystal structures of 4Pyr:DITFB, 4Pyr:TITFB, 4Pyr-Cl:TITFB and 4Pyr-Br:DITFB, the 'parent' −NH···N_2 was broken and halogen bonding occurred to both N_1 and N_2 pyridyl binding sites. In two out of four co-crystals, an N-H···O=C hydrogen bond was formed and in the other two cases an N-H···I interaction was observed. Since the N-H···I bond occurred in combination with TITFB (in 4Pyr:TITFB) and DITFB (in 4Pyr-Br:TITFB) it cannot be related to the type of co-former. Although there was no structure directing interaction at the carbonyl oxygen, in 4Pyr:TITFB, a red shift of 15 cm^{-1} was observed and with 4Pyr-Br:DITFB, a blue shift of 6 cm^{-1} occurred. All four co-crystals were accompanied by the emergence of an amide peak in the IR spectra. The N-H···O=C interaction in 4Pyr:DITFB was accompanied by a red shift of the carbonyl stretch of 15 cm^{-1} while in 4PyrCl:TITFB it was accompanied by a blue shift of 15 cm^{-1}.

Based on the interactions at the carbonyl group we can categorize the co-crystals into three groups; those which formed a N-H···O=C interaction, those in which an I···O=C interaction was present and those in which no interaction was shown at the carbonyl oxygen. The summarized data (Figure 9) indicate that an C-I···O=C did not bring about a significant change in the carbonyl peak and was comparable in value to when the target did not have any structure directing interactions at the carbonyl. On the other hand, NH···O=C did bring about bigger shifts to the carbonyl stretching mode (Figure 9).

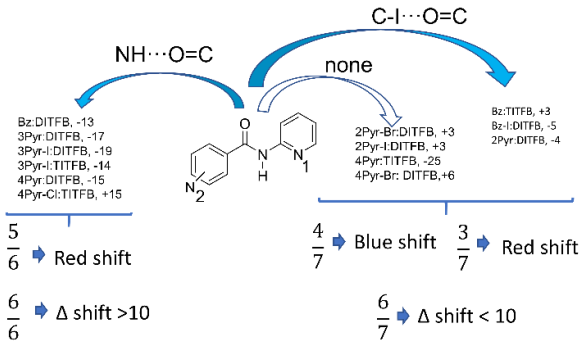

Figure 9. Summarized changes of carbonyl IR mode of co-crystal relative to respective target

Conclusion

A total of 13 co-crystals were analysed by SCXRD. In all three co-crystals obtained from the 2Pyr series the homomeric intramolecular HB −NH···N_2 remained intact. In the 10 co-crystals obtained from the other three series, the intermolecular HB found in the self-assembly of the target was broken in 9/10 times. In all co-crystals combined the interaction between XB donor and target was either to a N(pyr)=81%, O=C(15%) or π (4%). Finally, we note that an C-I···O=C does not bring about a significant change to the carbonyl stretch in comparison to when a NH···O=C hydrogen bond is present. Therefore, vibrational spectroscopy offers a very clear indication as to whether the carbonyl moiety acts as an acceptor for either a hydrogen- or a halogen bond or to neither.

Experimental Section

The target compounds were prepared as previously reported.[24] Co-crystal screening with the two halogen bond donors was carried out using liquid assisted grinding with stoichiometric 1:1 amounts of target and co-former, followed by IR characterization of the ground powder. A total of 32 experiments were performed. Peak shifts of ~3 cm^{-1} in several modes of both the target and co-former was used as the criterion to assess co-crystal formation paying special attention to peak shifts in amide (~3300-3400 cm^{-1}) and carbonyl regions (~1600-1700 cm^{-1}). IR spectra of co-crystal screening experiments were recorded with a Nicolet 380 FT-IR spectrometer using an attenuated total reflection (ATR) technique and ZnSe as the crystal. The melting points were measured using a Fisher-Johns melting point apparatus or a TA Instruments DSC Q20 differential scanning calorimeter. Datasets for single-crystal X-ray diffraction analysis were collected on a Bruker Kappa APEX II system (2Pyr-Br:DITFB, 2Pyr-I:DITFB, 3Pyr-I:DITFB) and a Rigaku XtaLAB Synergy-S (Bz:DITFB, Bz:TITFB, 2Pyr:TFB, 3Pyr:DITFB, 3Pyr-I:DITFB, 3Pyr-I:TITFB, 4Pyr:DITFB, 4Pyr:TITFB,4PyrCl:TITFB,4Pyr-Br:DITFB)

Deposition Number(s) 2065454 (for Bz:DITFB), 2065455 (for Bz:TITFB), 2065456 (for Bz-I:DITFB), 2065457 (for 2Pyr:DITFB), 2065458 (for 2Pyr-Br:DITFB), 2065459 (for 2Pyr-I:DITFB), 2065460 (for 3Pyr:DITFB), 2065461 (for 3Pyr-I:DITFB), 2065462 (for 3Pyr-I:TITFB), 2065463 (for 4Pyr:DITFB), 2065464 (for 4Pyr:TITFB), 2065465 (for 4Pyr-Cl:TITFB), 2065466 (for 4Pyr-Br:DITFB), contain(s) the supplementary crystallographic data for this paper. These data are provided free of charge by the joint Cambridge Crystallographic Data Centre and Fachinformationszentrum Karlsruhe Access Structures service www.ccdc.cam.ac.uk/structures

Acknowledgements

We acknowledge the NSF-MRI grant CHE-2018414, which was used to purchase a single-crystal X-ray diffractometer and associated software employed in this study. We are grateful to Dr. Victor W. Day at the University of Kansas for collecting some crystallographic data (NSF-MRI grant CHE-0923449).

Dr. Amila M. Abeysekera acknowledges support from the Johnson Cancer Research Center at Kansas State University, and The General Sir John Kotelawala Defence University, Sri Lanka.

Keywords: co-crystal • crystal engineering • halogen bonding • hydrogen bonding • supramolecular chemistry.

[1] S. H. Gellman, *Chem. Rev.* **1997**, *97*, 1231–1232.
[2] G. Berger, P. Frangville, F.Meyer, *ChemComm.* **2020**, *56*, 4970–4981.
[3] D. S María, M. A. Farrán, M. A. García, E. Pinilla, M. R. Torres, J. Elguero, R. M. Claramunt. *J. Org. Chem.* **2011**. *76*, 6780-6788.
[4] Y. M. Zhang, Q.Y. Xu, Y. Liu, *Sci. China: Chem.* **2019**, *62*, 549–560.
[5] P. Dervan, *Bioorg. Med. Chem.* **2001**, *9*, 2215–2235.
[6] K. B. Wang, J.Dickerhoff, G.Wu, D. Yang, *J. Am. Chem. Soc.* **2020***, 142*, 5204-5211
[7] A. Gautier, A. G.Tebo, *Curr. Opin. Chem. Bio.* **2020**, *57*, 58–64
[8] A. B. Grommet, L. M. Lee, R. Klajn, *Acc. Chem. Res.* **2020**, *53*, 2600–2610.
[9] H. Yamaguchi, R.Kobayashi, Y.Takashima, A. Hashidzume, A. Harada, *Macromolecules*. **2011**, *44*, 2395-2399.
[10] H. S. Chan, J. Kendrick, M. A. Neumann, F. J. Leusen, *CrystEngComm*. **2013**, *15,* 3799-3807.
[11] J. Zhou, G. Yu, F. Huang, *Chem. Soc. Rev.* **2017**, *46*, 7021–7053.
[12] H. R. Culver, J. R. Clegg, N. A. Peppas, *Acc. Chem. Res.* **2017**,*50*, 170-178.
[13] M. Jaegle, E. L.Wong, C. Tauber, E. Nawrotzky, C. Arkona, J. Rademann, *Angew. Chem, Int. Ed.* **2017**, *56*, 7358–7378.
[14] W. Chen, X. Tian, W. He, J. Li,; Y. Feng, G. Pan, *BMC Materials.* **2020**, *2*,1-22.
[15] H.Yao, H. Ke, X. Zhang, S. J. Pan, M. S. Li, L. P. Yang, G. Schreckenbach, W. Jiang, *J. Am. Chem. Soc.* **2018,** *140*, 13466-13477.
[16] G. R. Desiraju, *Angew Chem Int Ed*. **2007**,*46*, 8342-8356.
[17] C. V. Krishnamohan Sharma, *Cryst. Growth. Des.* **2002**, 2, 465-474.
[18] T. Steiner, *Angew. Chem, Int. Ed.* **2002,** *41*, 48-76.
[19]C. B Aakeröy, K. R. Seddon, *Chem. Soc. Rev*. **1993**, 22, 397-407.
[20] G. R. Desiraju, P. S. Ho, L. Kloo, A. C. Legon, R. Marquardt, P. Metrangolo, P. Politzer, G. Resnati, K. Rissanen, *Pure Appl. Chem.* **2013**, *85*, 1711-1713
[21] I. Alkorta, J. Elguero, A. Frontera, *Crystals.* **2020**, *10*, 180.
[22] K. E. Riley, *Chem. Phys. Lett.* **2020**, *744*, 137221.
[23] S. M. Huber, J. D. Scanlon, E. Jimenez-Izal, J. M. Ugalde, I. Infante, *Phys. Chem. Chem. Phys.* **2013**, *15*, 10350–10357.
[24] A. M. Abeysekera, V. W. Day, A. S. Sinha, C. B. Aakeröy, *Cryst. Growth Des.* **2020**, 20, 7399-7410
[25] Y.V. Torubaev, I. V. Skabitsky, *CrystEngComm.* **2019**, *21*, 7057–7068.
[26] M. C. Pfrunder, A. S. Micallef, L. Rintoul, D. P. Arnold, K. J. Davy, J. McMurtrie, *Cryst. Growth Des.* **2014** *14*, 6041-6047.
[27] M.Vartanian, A. C. B. Lucassen, L. J. W. Shimon, M. E. van der Boom, *Cryst. Growth Des.* **2008**, *8*, 786–790.
[28] M. D. Perera, J. Desper, A. S. Sinha, C. B. Aakeröy, *CrystEngComm.* **2016**, *18*, 8631–8636.
[29] C. B. Aakeröy, T. K. Wijethunga, J.Desper, C. Moore, *J. Chem. Crystallogr.* **2015**, *45*, 267–276.
[30] A. C. Lucassen, A. Karton, G. Leitus, L. J. Shimon, J. M. Martin, M. E. Van Der Boom, *Cryst. Growth Des.***2007***, 7*, 386-392.
[31] I. Nicolas, F. Barrière, O. Jeannin, M. Fourmigué, *Cryst. Growth Des.* **2016,** *16*, 2963-2971.
[32] L. C. Roper, C. Prasang, V. N. Kozhevnikov, A. C. Whitwood, P. B. Karadakov, D. W. Bruce, *Cryst. Growth Des*. **2010**, *10*, 3710-3720.
[33] H. R. Khavasi, A. A. Tehrani, *CrystEngComm.* **2013**, *15*, 3222–3235.
[34] P. Metrangolo, G. Resnati, *IUCrJ.* **2014**, *1* (Pt 1), 5–7.
[35] M.R. Scholfield, C.M.V.Zanden, M. Carter, P.S. Ho, *Protein Sci.* **2013**, *22*, 139-152.
[36]A. M. S. Riel, D. A. Decato, J. Sun, C. J. Massena, M. J. Jessop, O. B. Berryman, *Chem.* **2018**, *9*, 5828-5836.
[37] A. M. S. Riel, R. K. Rowe, E. N. Ho, A. C. C. Carlsson, A. K. Rappé, O. B. Berryman, P.S. Ho, *Acc. Chem. Res*. **2019**, *52*, 2870-2880.
[38] A.Takemura, L. J. McAllister, S. Hart, N. E. Pridmore, P.B.Karadakov, A. C. Whitwood, D. W. Bruce,*Chemistry (Weinheim an der Bergstrasse, Germany)*. **2014**, *20*, 6721.
[39] A. Takemura, L. J. McAllister, P. B. Karadakov, N. E. Pridmore, A. C. Whitwood, A., W.D. Bruce, *CrystEngComm*, **2014**, *16*, 4254-4264.
[40] C. B Aakeröy, M. Fasulo, N Schultheiss, J. Desper, J, C. Moore, *J. Am. Chem. Soc.* **2007**,*129*,13772-13773.

Entry for the Table of Contents

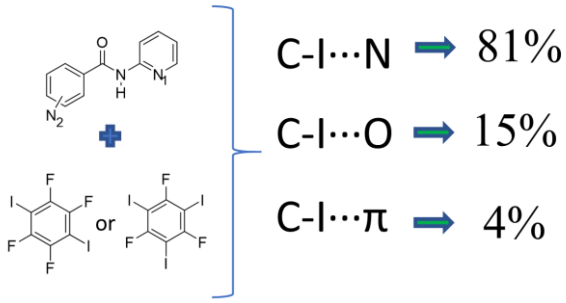

A series of co-crystallization experiments with halogen bond donors and sixteen target molecules were carried out to map preferred binding sites of halogen-bond donors, and it was found to be in the order of π (4%) < O=C(15%) < N(pyr)=81%.